Carcinogenesis vol.30 no.5 pp.745–752, 2009
doi:10.1093/carcin/bgp061
Advance Access publication March 11, 2009

Ceramide synthases and ceramide levels are increased in breast cancer tissue

Susanne Schiffmann*,†, Jessica Sandner†, Kerstin Birod, Ivonne Wobst, Carlo Angioni, Eugen Ruckhäberle[1], Manfred Kaufmann[1], Hanns Ackermann[2], Jörn Lötsch, Helmut Schmidt, Gerd Geisslinger and Sabine Grösch

*pharmazentrum frankfurt/*ZAFES, Institute of Clinical Pharmacology, [1]Department of Gynecology and [2]Institute of Biomathematics, Goethe-University, Theodor-Stern-Kai 7, 60590 Frankfurt am Main, Germany

*To whom correspondence should be addressed. Tel: +49 69 6301 7820; Fax: +49 69 6301 7636;
Email: susanne.schiffmann@med.uni-frankfurt.de

Several *in vitro* studies have correlated dysfunction of the sphingolipid-signaling pathway with promotion of tumor cell growth as well as progression and resistance of tumors to chemotherapeutic agents. As ceramides (Cer) constitute the structural backbones of all sphingolipids, we investigated the endogenous ceramide levels in 43 malignant breast tumors and 21 benign breast biopsies and compared them with those of normal tissues using liquid chromatography coupled with tandem mass spectrometry (LC-MS/MS). The total ceramide levels in malignant tumor tissue samples were statistically significantly elevated when compared with normal tissue samples. Upregulation of the total ceramide level averaged 12-fold and 4-fold higher than normal tissue samples, for malignant tumors and benign tissues, respectively. Specifically, the levels of $C_{16:0}$-Cer, $C_{24:1}$-Cer and $C_{24:0}$-Cer were significantly raised in malignant tumors as compared with benign and normal tissue. The augmentation of the various ceramides could be assigned to an increase of the messenger RNA levels of ceramide synthases (CerS) LASS2 (longevity assurance), LASS4 and LASS6. Notably, elevated levels of $C_{16:0}$-Cer were associated with a positive lymph node status, indicating a metastatic potential for this ceramide. Moreover, the levels of $C_{18:0}$-Cer and $C_{20:0}$-Cer were significantly higher in estrogen receptor (ER) positive tumor tissues as compared with ER negative tumor tissues. In conclusion, progression in breast cancer is associated with increased ceramide levels due to an upregulation of specific LASS genes.

Introduction

Sphingolipids regulate various cellular processes linked to cancer development, progression, metastasis and resistance to therapy (1,2). Sphingolipids are synthesized *de novo* at the endoplasmic reticulum from serine and palmitoyl-CoA, which condense to form 3-ketosphinganine through the action of L-serine palmitoyl-CoA transferase (SPT), followed by rapid reduction to sphinganine (dhSph) by the 3-ketosphinganine reductase. Acyl-CoAs with various chain lengths are attached to sphinganine by chain length specific (dihydro)ceramide synthases (LASS1–6) [3] and dihydroceramide desaturase (DEGS) converts dihydroceramides (dhCer) to ceramides (Cers). The enzymes ceramidase and sphingosine kinase (SphK) 1 and 2 metabolize ceramides via sphingosine (Sph) to sphingosine-1-phosphate (S1P) (Figure 1).

The biologically active sphingolipids ceramide, Sph and dhSph play important and general roles in cellular regulation, such as apoptosis, cell cycle arrest and senescence (4). Furthermore, some glycosylated (glycosylceramide) or phosphorylated (ceramide 1-phosphate) metabolites of ceramides are involved in signal transduction pathways leading to either inhibition of apoptosis or promotion of cell growth (5,6). Elevated glycosphingolipids (gangliosides) also correlate with augmented tumor invasiveness (7). In contrast, S1P has a diverse role in signaling that depends on the synthesizing enzymes (SphK1 and SphK2) as well as the subcellular place of origin. S1P synthesized by SphK1 is involved in proliferative signaling (8), whereas S1P synthesized by SphK2 is described as an antiproliferative and apoptotic mediator (9). We recently observed contrasting data for the role of SphK2, in which MCF-7-SphK2-silenced xenografts grew slower in nude mice as compared with MCF-7-SphK2 wild-type xenografts (A.Weigert, S.Schiffmann, D.Sekar, S.Ley, S.Grösch, G.Geisslinger and B.Brüne submitted for publication).

Previous studies described different expression profiles of the sphingolipid metabolic enzymes in cancerous tissue relative to normal tissue. Kawamori *et al.* (10) and Johnson *et al.* (11) observed an upregulation of SphK1 in rat colon adenocarcinoma and lung cancer. A relevant role for SphK1 in carcinogenesis has also been shown in human prostate and breast cancer cells (12–14). Furthermore, in human astrocytoma grade 4 tissue, the overexpression of SphK1, but not SphK2, correlates with poor patient survival (15). In human prostate tumor tissues, the level of acid ceramidase is variable and seems to be relevant for proliferation, migration and as well as resistance to several chemotherapeutics (16,17). Koybasi *et al.* detected decreased LASS1 expression in human head and neck squamous cell carcinomas. In contrast, overexpression of LASS1 in head and neck squamous cell carcinomas cells leads to an increase of $C_{18:0}$-Cer and subsequently to an inhibition of cell proliferation (18). Taken together, these data indicate that enzymes of the sphingolipid metabolism such as SphK1, ceramidase and CerSs are involved in carcinogenesis in various tissues (colon, breast, prostate, head and neck). Alterations in the expression profile may be reflected in an altered sphingolipid level. Additionally, recent studies implied a distinct role for the ceramide *N*-acyl chain length, indicating that ceramides containing specific fatty acids play defined roles in cell physiology (19–22). In this study, we investigated the endogenous sphingolipid levels in breast cancer and normal tissue samples on both the transcriptional and/or translational levels.

Abbreviations: Cer, ceramide; CerS, (dihydro)ceramide synthase; dhCer, dihydroceramide; dhSph, sphinganine; ER, estrogen receptor; GAPDH, glyceraldehyde-3-phosphate dehydrogenase; LASS, longevity assurance homolog; LN, lymph node; mRNA, messenger RNA; S1P, sphingosine-1-phosphate; Sph, sphingosine; SphK, sphingosine kinase; SPT, L-serine palmitoyl-CoA transferase; SPTLC, L-serine palmitoyl-CoA transferase long chain.

†These authors contributed equally to this work.

Materials and methods

Reagents

The sphingolipid standards were purchased either from Avanti Polar Lipids (Alabaster, AL) or Matreya LLC (Pleasant Gap, PA). The antibodies LASS1 (goat polyclonal), LASS2 (goat polyclonal), LASS3 (goat polyclonal), LASS4 (goat polyclonal), LASS5 (goat polyclonal), SPT (goat polyclonal) and LASS6 (mouse monoclonal) were obtained from Santa Cruz Biotechnology (Heidelberg, Germany) and from Abnova GmbH (Heidelberg, Germany), whereas glyceraldehyde-3-phosphate dehydrogenase (GAPDH) (mouse monoclonal) was obtained from Applied Biosystems/Ambion (Austin, TX).

Tissue samples

Malignant tissue, benign tissue and normal tissues of breast cancer patients were collected over 7 years with informed consent from patients undergoing surgical resection from the Department of Gynecology (Goethe-University, Frankfurt/Main, Germany). The protocol was approved from the local ethics committee. The samples were taken in the years 2001, 2003, 2005, 2006 and 2007. All tissue samples were stored at −80°C. Normal tissues (not benign, not malignant) were excised at least 1 cm away from the main tumor mass of the patients, but the tumor tissues from these patients were not included in this study. Therefore, the tumor tissues and the normal tissues originate from different patients (unpaired samples). Breast tissue samples were characterized according to standard pathology based on the estrogen receptor (ER) status as determined by ligand binding assays or by immunohistochemistry.

Determination of sphingolipid concentrations in tissue

Tissue samples (5–15 mg) used for quantification of sphingolipid concentrations were minced in phosphate-buffered saline on ice. A 10 µl tissue

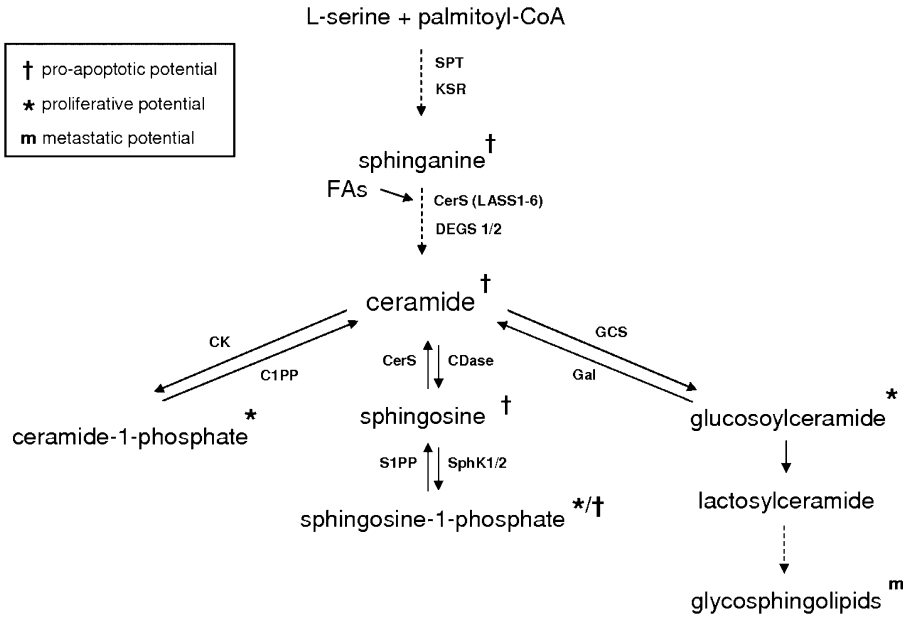

Fig. 1. Sphingolipid pathway. The various sphingolipids exhibit proapoptotic (†), proliferative (*) or metastatic (m) potential. The symbols '*/†' indicate that S1P exhibits proliferative as well as proapoptotic potency depending on the location where it is synthesized as well as on the synthesizing enzyme (SphK1 or SphK2). CDase, ceramidase; CK, ceramide kinase; C1PP, ceramide-1-phosphate phosphatase; DEGS, dihydroceramide desaturase; FA, fatty acid; Gal, galactosidase, GCS, glucosylceramide synthase; KSR, 3-ketosphinganine reductase; SK1/2, sphingosine kinase1/2; S1PP, sphingosine-1-phosphate phosphatase.

suspension (0.03 mg/μl) was added to 90 μl of freshly prechilled phosphate-buffered saline. Lipids were extracted in 700 μl of chloroform:methanol (7:1) after the addition of the internal standards ($C_{17:0}$-Cer, $C_{17:0}$-Sph, $C_{17:0}$-S1P). The suspension was vortexed at 25°C for 1 min and centrifuged for 5 min at 25°C and 14 000 r.p.m. The organic phase was collected and the extraction step was repeated. The combined organic phases were dried under a stream of nitrogen and redissolved in 200 μl of methanol for quantitation. After liquid–liquid extraction, concentrations of $C_{16:0}$-Cer, $C_{18:0}$-Cer, $C_{20:0}$-Cer, $C_{24:1}$-Cer and $C_{24:0}$-Cer and the internal standards were determined by liquid chromatography coupled with tandem mass spectrometry as described previously (23). Chromatographic separation was accomplished under gradient conditions using a Luna C18 column (150 × 2 mm ID, 5 μm particle size and 10 nm pore size; Phenomenex, Aschaffenburg, Germany). Precursor to product ion transitions of m/z 538 →264 for $C_{16:0}$-Cer, of m/z 566 →264 for $C_{18:0}$-Cer, of m/z 594 →264 for $C_{20:0}$-Cer, of m/z 648 →264 for $C_{24:1}$-Cer, of m/z 651 →264 for $C_{24:0}$-Cer, of m/z 540 →284 for $C_{16:0}$-dhCer, of m/z 568 →284 for $C_{18:0}$-dhCer, of m/z 596 →284 for $C_{20:0}$-dhCer,of m/z 651 →284 for $C_{24:1}$-dhCer, of m/z 653 →284 for $C_{24:0}$-dhCer, of m/z 300 →282 for Sph, of m/z 302 →284 for dhSph, of m/z 380 →264 for Sph1P, of m/z 382 →266 for sphinganine-1-phosphate, of m/z 552→534 for $C_{17:0}$-Cer, of m/z 286→268 for $C_{17:0}$-Sph and of m/z 366→250 for $C_{17:0}$-Sph1P were used for the multiple reaction monitoring with a dwell time of 15 ms. The concentrations of Sph, dhSph, S1P and sphinganine-1-phosphate in the selected tumor volume were below the detection limit. The tumor volume could not be scaled up due to the priority for pathological studies that required a greater part of sample. Concentrations of the calibration standards, quality controls and unknowns were evaluated by Analyst software 1.4.2 (Applied Biosystems). A representative chromatogram of $C_{16:0}$-Cer, $C_{17:0}$-Cer, $C_{18:0}$-Cer, $C_{20:0}$-Cer, $C_{24:1}$-Cer and $C_{24:0}$-Cer is displayed in supplement 1 (available at *Carcinogenesis* Online). Suppression effects were assessed by extraction of tissue samples that were supplemented with 10 ng/ml internal standard in methanol. The mean peak areas of the samples supplemented with internal standard were compared with the mean peak area of the internal standard in methanol. An ion suppression effect was observed between 15 and 25% for the internal standard. Linearity of the calibration curve was proven for $C_{16:0}$-Cer from 2 to 1000 ng/ml (3.7–1857 pmol/ml), for $C_{18:0}$-Cer from 0.3 to 150 ng/ml (0.53–265 pmol/ml), for $C_{20:0}$-Cer from 0.4 to 200 ng/ml (0.67–336 pmol/ml), for $C_{24:1}$-Cer from 0.8 to 400 ng/ml (1.2–620 pmol/ml) and for $C_{24:0}$-Cer from 1 to 1000 ng/ml (1.54–1537 pmol/ml). The coefficient of correlation for all measured sequences was at least 0.99. Variations in accuracy and intraday and interday precision ($n = 2$ for each concentration in breast tissue) were <15% over the whole range of calibration.

Real-time quantitative polymerase chain reaction

Tumor tissue of patients with elevated and normal sphingolipid levels was investigated. The messenger RNA (mRNA) was isolated using a RNA isolation kit (Qiagen, Hilden, Germany) according to the manufacturer's instructions, with an optional DNAse step. Complementary DNA synthesis was performed using 200 ng mRNA and random hexamers of the Superscript III kit (Invitrogen GmbH, Karlsruhe, Germany). The expression levels of LASS1–6 and SPT were determined by Taqman™ analysis using SYBR Green kit (AbGene Limited, Epsom, UK) with an ABI Prism 7500 Sequence Detection System (Applied Biosystems). Relative expression of L-serine palmitoyl-CoA transferase long chain subunit 2 (SPTLC2) and CerS family genes was determined using the comparative cycle threshold method, normalizing relative values to the average expression of β-actin and GAPDH as housekeeping genes (24). The designed primer sets were listed in supplement 2 (available at *Carcinogenesis* Online). Linearity of the assays was determined by serial dilutions of the templates for each primer set separately.

Western blot analysis

Frozen tissue was chopped with a mortar, suspended in lysate buffer [150 mM NaCl, 50 mM Tris, 1% NP40, 1% sodium deoxycholate, 0.1% sodium dodecyl sulfate, 1% Triton-X 100, Roche complete (Roche, Mannheim, Germany) pH 7.4], sonicated and centrifuged (14 000*g*, 10 min, 4°C). The supernatant was stored at −80°C. Forty micrograms of the protein lysate were electroblotted. The antibodies used were diluted as follows: LASS1, 3, 4, 5, 6, SPT (1:100); LASS2 (1:300) and GAPDH (1:2000).

Statistical analysis

First, the tissue concentrations of the various ceramides were compared by means of Friedman analysis of variance, with post-hoc Wilcoxon–Wilcox comparisons, α-corrected for multiple testing according to Bonferroni (BIAS software version 8.4, http://www.bias-onlinede.). Second, to analyze whether or not the ceramide concentrations differed between the tissue type subgroups (malignant, benign and normal), ceramide concentrations were submitted to Kruskal–Wallis analysis (25), with the post-hoc α-corrected Dunn testing, separately for each ceramide. Third, at an exploratory level, ceramide tissue concentrations in the tumor type subgroups (malignant/benign) were compared between samples with respect to tumor size (large or small) by means of Kruskal–Wallis analysis (25), with the post-hoc α-corrected Dunn testing, separately for each ceramide. Furthermore, also at an exploratory level, ceramide tissue concentrations in the malignant tissue subgroup were compared between samples with respect to lymph node (LN) status (positive or negative) and ER status (positive or negative) by means of Mann–Whitney *U* tests,

separately for each ceramide. Fourth, ceramide tissue concentrations were analyzed for correlations with SPT and LASS mRNA quantities using Spearman's ρ correlation analysis.

Results

Ceramide distribution in normal breast tissue

The aim of the study was to compare the endogenous ceramide levels in malignant and benign tissue with normal tissue to gain insight into the importance of ceramide deregulation in cancer development. Ceramide synthases act chain length specific. Therefore, we investigated ceramides of varying chain lengths in malignant, benign and normal tissues by liquid chromatography coupled with tandem mass spectrometry. To present a representative sphingolipid level, three to five different pieces of the tissue samples were employed and the sphingolipid level of each of these pieces was analyzed in duplicate. Figure 2 displays the mean ceramide levels of normal breast tissue normalized to 1 mg tissue ($n = 12$). The Friedman test showed that the concentration of the various ceramides differ in part significantly from each other. It is obvious that $C_{16:0}$-Cer [9.40 ± 2.8 (pmol/mg)], $C_{24:1}$-Cer [2.80 ± 0.8 (pmol/mg)] and $C_{24:0}$-Cer [3.49 ± 0.9 (pmol/mg)] are the predominant ceramides in healthy breast tissue. The concentrations of Sph, dhSph, S1P and sphinganine-1-phosphate were under the detection limit in the selected tissue sample.

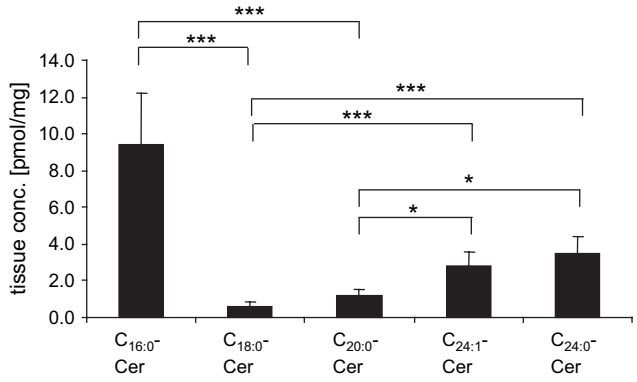

Fig. 2. Ceramide levels in breast normal tissue. The normal tissue was obtained as described in Materials and Methods. The sphingolipid amounts determined by liquid chromatography coupled with tandem mass spectrometry were related to the weight of the investigated tissue. The values are the mean of at least three values of different parts of the tumor tissue and each experiment was achieved in duplicate. The mean value is shown by a horizontal line. The statistical analysis was done by Wilcoxon–Wilcox test (Bonferroni α-corrected). $^{*}P < 0.05$ and $^{***}P < 0.001$ indicate significant difference among the various ceramides.

Analysis of ceramide levels of malignant, benign and normal breast tissue

The levels of endogenous ceramides in 64 breast tumor tissues [malignant ($n = 43$); benign ($n = 21$)] were measured and compared with 12 samples of normal tissues. Malignant tumor tissues comprise the invasive breast cancer types 'invasive lobar mamma carcinoma' and 'invasive ductal mamma carcinoma' and the pre-stage breast cancer types 'lobar carcinoma *in situ*' and 'ductal carcinoma *in situ*'. The benign tissues include mastopathies and fibroadenomas. Figure 3A and Table I clearly exhibit that the total ceramide levels were significantly increased in malignant tissue as compared with the benign tissue and the normal tissue. The ceramide levels in the benign tissue were also increased as compared with normal tissue. A significant increase of ceramide levels in malignant tumor tissue versus the benign tissue points to a positive correlation of the ceramide level and disease severity (Table I). An increase in ceramide levels in malignant and benign tissue versus normal tissue was observed for: $C_{16:0}$-Cer, $C_{18:0}$-Cer, $C_{20:0}$-Cer, $C_{24:0}$-Cer and $C_{24:1}$-Cer (Table I).

Next, we determined the extent to which ceramides were increased in tumor tissues. For this purpose, we related the mean values (for each specific ceramide) of the malignant and the benign samples to the corresponding mean value of the normal samples. The total ceramide level in malignant (benign) tumor tissue was 12.0-fold (4.0-fold) increased compared to normal tissue. The ceramide specific increase varied: 14.5-fold/4.4-fold (malignant/benign) for $C_{16:0}$-Cer, 5.2-fold/5.1-fold for $C_{18:0}$-Cer, 5.6-fold/3.9-fold for $C_{20:0}$-Cer, 5.9-fold/2.3-fold for $C_{24:1}$-Cer and 10.7-fold/3.5-fold for $C_{24:0}$-Cer, respectively (Figure 3B). These data indicate that in malignant tumors the elevation of $C_{16:0}$-Cer, $C_{24:1}$-Cer and $C_{24:0}$-Cer concentrations were more pronounced than that of other ceramides (Table 1).

Comparison of sphingolipid level and pathological parameters

To gain insight into the prognostic significance of the sphingolipid level, we investigated whether or not a relationship exists between an elevated sphingolipid level and various pathological parameters such as tumor size, LN status and hormone receptor status. The pathological parameters were not available for all patients, subgroups of patients from which the investigated parameters are known were selected. We missed the information concerning the tumor size of

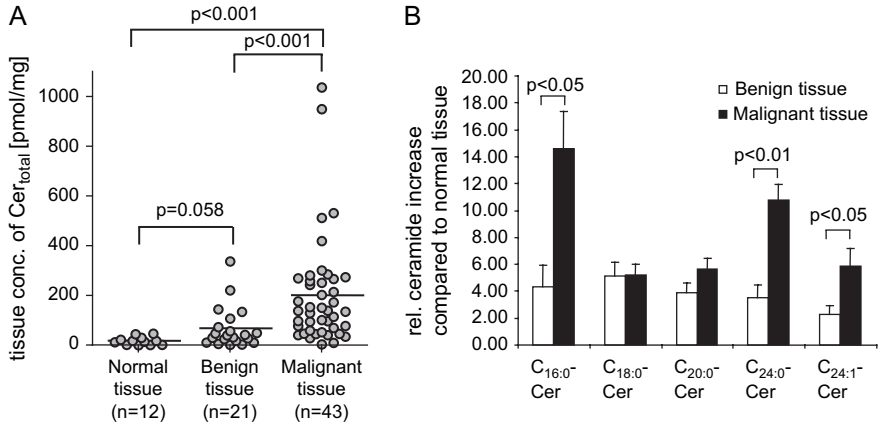

Fig. 3. (**A**) Distribution of the total ceramide levels of malignant, benign and normal tissue of the breast. The tissues were obtained as described in Materials and Methods. The sphingolipid amounts determined by liquid chromatography coupled with tandem mass spectrometry were related to the weight of the investigated tissue. Every point (result of one patient) consists of the mean of three to five values of different parts of the tumor and each experiment was achieved in duplicate. The mean value is shown by a horizontal line. The statistical analysis was done by Kruskal–Wallis analysis with the post-hoc α-corrected Dunn testing. *P* indicates significant difference between the various tumor types and the normal tissue samples. (**B**) Relative ceramide increase in benign and malignant breast tissues compared with normal breast tissues. The specific ceramide levels of benign and malignant tissues were related to the specific ceramide levels of normal tissues.

Table I. Ceramide levels of all samples (normal tissue, benign tissue and malignant tumor tissue) and of the subgroups tumor size, LN status, ER status and HER-2/neu status are shown

	Number of patients	Cer_{total} (pmol/mg tissue)	$C_{16:0}$-Cer (pmol/mg tissue)	$C_{18:0}$-Cer (pmol/mg tissue)	$C_{20:0}$-Cer (pmol/mg tissue)	$C_{24:1}$-Cer (pmol/mg tissue)	$C_{24:0}$-Cer (pmol/mg tissue)
ALL							
Normal	12	17.47 ± 4.7	9.40 ± 2.8	0.61 ± 0.2	1.17 ± 0.3	2.80 ± 0.8	3.79 ± 0.9
Benign tissue	21	67.43 ± 18.6	41.0 ± 15.5	3.12 ± 0.7	4.56 ± 0.8	6.42 ± 1.7	12.38 ± 3.2
Malignant tissue	43	200.66 ± 31.7	137.01 ± 26.4	3.16 ± 0.5	6.58 ± 1.0	16.40 ± 3.6	37.50 ± 4.1
Tumor size							
Benign tissue							
≤2 cm	7	15.70 ± 6.0	6.32 ± 2.9	0.90 ± 0.4	1.57 ± 0.7	2.11 ± 1.0	4.80 ± 2.2
>2 cm	10	88.00 ± 30.4	46.55 ± 25.9	5.08 ± 1.0	6.60 ± 1.1	9.11 ± 3.0	20.70 ± 5.0
Malignant tissue							
≤2 cm	21	155.78 ± 22.1	96.80 ± 17.6	2.62 ± 0.5	5.77 ± 0.9	11.9 ± 1.8	38.77 ± 6.9
>2 cm	20	207.70 ± 55.4	141.62 ± 44.5	3.52 ± 0.9	7.05 ± 1.8	18.32 ± 7.3	37.18 ± 5.9
LN status							
negative	24	131.18 ± 24.2	81.98 ± 20.7	2.49 ± 0.5	4.99 ± 0.9	10.60 ± 3.9	31.12 ± 3.9
positive	16	254.90 ± 62.8	175.02 ± 49.5	3.62 ± 1.0	8.13 ± 2.1	20.95 ± 9.1	47.18 ± 9.9
ER status							
negative	18	137.53 ± 28.9	84.75 ± 22.3	1.44 ± 0.2	3.89 ± 0.8	9.72 ± 1.3	37.71 ± 8.3
positive	20	216.53 ± 61.9	143.60 ± 49.8	4.26 ± 0.9	8.50 ± 1.8	21.09 ± 8.0	39.08 ± 5.3
HER-2/neu status							
negative	21	116.89 ± 23.8	62.30 ± 17.8	2.60 ± 0.6	5.11 ± 1.0	9.94 ± 2.0	36.94 ± 5.9
positive	10	225.67 ± 85.2	168.31 ± 75.6	3.1 ± 0.9	6.34 ± 1.8	17.66 ± 6.9	30.26 ± 4.7

The ceramide levels are shown as mean ± SEM. The pathological parameters were not available for all patients. Those patients whose investigated parameters are known were selected. The number of patients that were analyzed is stated in column 2. Data were statistically analyzed using Kruskal–Wallis test with the post-hoc α-corrected Dunn test or the Mann–Whitney *U* test ($^{*}P < 0.05$, $^{**}P < 0.01$, $^{***}P < 0.001$). The samples that were compared with each other were marked with parentheses.

six patients, the LN status of three patients, the ER status of five patients and the human epidermal growth factor receptor (HER-2/neu) status of 12 patients. The number of patients that were analyzed is given in parentheses.

Tumor size: To exclude the possibility that the raised ceramide levels were a result of necrosis (mainly occurring in larger tumors), we compared the total ceramide levels of malignant and benign tissue with a diameter >2 cm ($n = 20$) or ≤2 cm ($n = 21$) (supplement 3A is available at *Carcinogenesis* Online). Malignant tumors disclose no significant correlation between tumor size and ceramide level, indicating that necrosis is not responsible for the raised ceramide level. In contrast, malignant tumors independent of tumor size and benign tumors with a diameter >2 cm ($n = 10$) show a significant increase in ceramide level in comparison with benign tumors with smaller dimensions ($n = 7$) (Table I, supplement 3A is available at *Carcinogenesis* Online). These data indicate that the increased ceramide level correlates with disease severity.

LN status: A metastatic potential in colon cancer is discussed in the literature (26) for glycosylated ceramides. Therefore, we investigated whether an elevated ceramide level in tumors could be linked to the LN status. For malignant tumor tissue, the LN status was known from 40 patients [positive LN ($n = 16$); negative LN ($n = 24$)]. Figure 4A displays that the median of the total ceramide level, and specifically of $C_{16:0}$-Cer, $C_{24:1}$-Cer and $C_{24:0}$-Cer, was increased in tumor tissues from patients with a positive LN status as compared with tumor tissues from patients with a negative LN status, whereas $C_{18:0}$-Cer and $C_{20:0}$-Cer were nearly unchanged. Interestingly, the increase of $C_{16:0}$-Cer was significant. (Figure 4A, Table I).

Grading status: Next, we investigated whether another important pathological parameter, the grading status of the malignant tumors, could be related to the sphingolipid status of the tumors. There was no significant difference between the ceramide levels of malignant tumor tissue ascribed to the G1–G2 status ($n = 23$) and to malignant tumors ascribed to the G3–G4 status ($n = 20$) (data not shown).

ER and HER-2/neu status: Since the ER and the HER-2/neu status have important clinical implications in breast cancer, we checked whether the ceramide level could be linked to the ER or HER-2/neu receptor status. $C_{18:0}$-Cer and $C_{20:0}$-Cer are significantly elevated in ER positive malignant tumors, whereas $C_{16:0}$-Cer, $C_{24:0}$-Cer and $C_{24:1}$-Cer are independent of the ER status (Figure 4B). However, the observed ceramide increase in malignant tumor tissue is independent of the HER-2/neu status (Table I). There was also no correlation between the various ceramide levels of malignant tumors and a HER-2/neu negative/ER negative status (data not shown).

The mRNA expression levels of SPT and LASS1–6 in breast tumor tissue

In order to obtain insight into the enzymes of the sphingolipid pathway that contribute to the elevated ceramide levels, the mRNA levels of all ceramide synthases (LASS1–6) and SPT (see also Figure 1) were investigated using real-time quantitative polymerase chain reaction. The SPT consists of at least two subunits SPTLC1/SPTLC2. Both subunits are equally expressed in breast tissue (27). Recently, a new subunit of the SPT, SPTLC3, with variable tissue expression was described (28). We therefore investigated the mRNA level of both SPTLC2 and SPTLC3. We examined 10 samples of tumor tissues with elevated ($n = 4$) and depressed ($n = 6$) sphingolipid levels. The mRNA expression level of each LASS and SPT were normalized to the average expression level of ß-actin and GAPDH (supplement 4 is available at *Carcinogenesis* Online). The mRNA level of LASS1, LASS3 and SPTLC3 were below the quantification limit. The functionality of the primers, which were used for the quantitative polymerase chain reaction of LASS1 and LASS3 in the breast tumor tissue were tested with brain and prostate tissue as positive controls, where LASS1 and LASS3 are predominantly expressed (29–31). The specific ceramide levels were plotted against the various LASS and

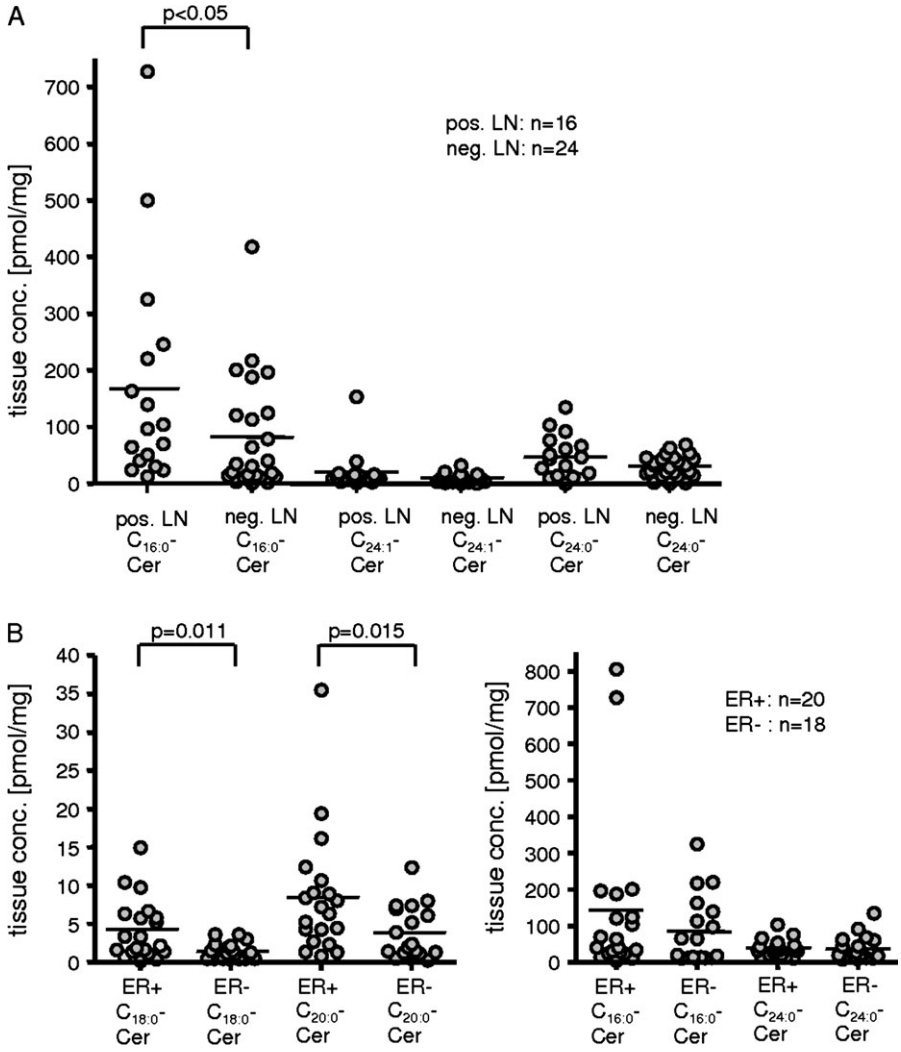

Fig. 4. Ceramide levels of malignant tumor tissues in dependency on the LN status (**A**) and on the ER status (**B**). The sphingolipid amounts determined by liquid chromatography coupled with tandem mass spectrometry were related to the weight of the investigated tissue. Every point (result of one patient) consists of the mean of three to five values of different parts of the tumor mass and each experiment was achieved in duplicate. The mean value is shown by a horizontal line. The statistical analysis was done by the Mann–Whitney *U* test. *P* indicates a significant difference in malignant tissue between positive LN status/ER status and negative LN status/ER status.

SPTLC2 mRNA levels, respectively. Figure 5A–D shows exemplarily the scatter plots for LASS2 against $C_{16:0}$-Cer and $C_{24:1}$-Cer and LASS6 against $C_{18:0}$-Cer and $C_{20:0}$-Cer, respectively. Figure 5E presents the Spearman's rank correlation coefficient of all data. We observed a significant correlation between LASS2/$C_{16:0}$-Cer (r_{sp} = 0.77, P = 0.009), LASS4/$C_{18:0}$-Cer (r_{sp} = 0.65, P = 0.042), LASS6/$C_{18:0}$-Cer (r_{sp} = 0.74, P = 0.014), LASS4/$C_{20:0}$-Cer (r_{sp} = 0.68, P = 0.030), LASS6/$C_{20:0}$-Cer (r_{sp} = 0.84, P = 0.002), LASS2/$C_{24:1}$-Cer (r_{sp} = 0.72, P = 0.019), LASS6/$C_{24:1}$-Cer (r_{sp} = 0.64, P = 0.047) and LASS2/$C_{24:0}$-Cer (r_{sp} = 0.71, P = 0.022). There was no correlation between ceramide level and SPTLC2 mRNA level. However, SPTLC2 and LASS5 were elevated in patients 1 and 2, which exhibited an outstanding increased ceramide level (supplement 4 is available at *Carcinogenesis* Online).

The protein expression level of SPT and LASS in breast tumor tissue

Next, we analyzed whether translational modifications also play a role in the altered sphingolipid level in cancerous tissue using western blot analysis. Unfortunately, the currently available antibodies of LASS1, LASS3, LASS4, LASS5, LASS6 and SPT are not specific; therefore, no reproducible western blot or immunohistochemical staining was obtainable. Only LASS2 was reasonably detectable (supplement 5B is available at *Carcinogenesis* Online). Tissue samples that were previously subjected to the expression analysis of the mRNA level were used for the determination of the protein expression level. Using histochemistry, we showed that the investigated tumor tissues consist predominantly of one cell type (supplement 5A is available at *Carcinogenesis* Online); therefore, we could exclude cell type specific differences in the expression pattern of the LASS's. The western blot analysis revealed a correlation between ceramide level and LASS2 expression (supplement 5B is available at *Carcinogenesis* Online).

Discussion

In this study, we could clearly show that the total endogenous ceramide level was significantly elevated in malignant (12-fold) and benign (4-fold) breast tissue as compared with normal tissue, indicating that elevation of sphingolipid levels correlates with disease status. This elevation in ceramide levels was rather unexpected because *in vitro* studies predominantly indicated that an increase in ceramides is associated with an induction of apoptosis and therefore primarily linked with anticarcinogenic effects. An elevated concentration of sphingomyelin, a metabolite of ceramide, was also observed in human cancerous cervical tissues compared with normal cervical tissue (32). In

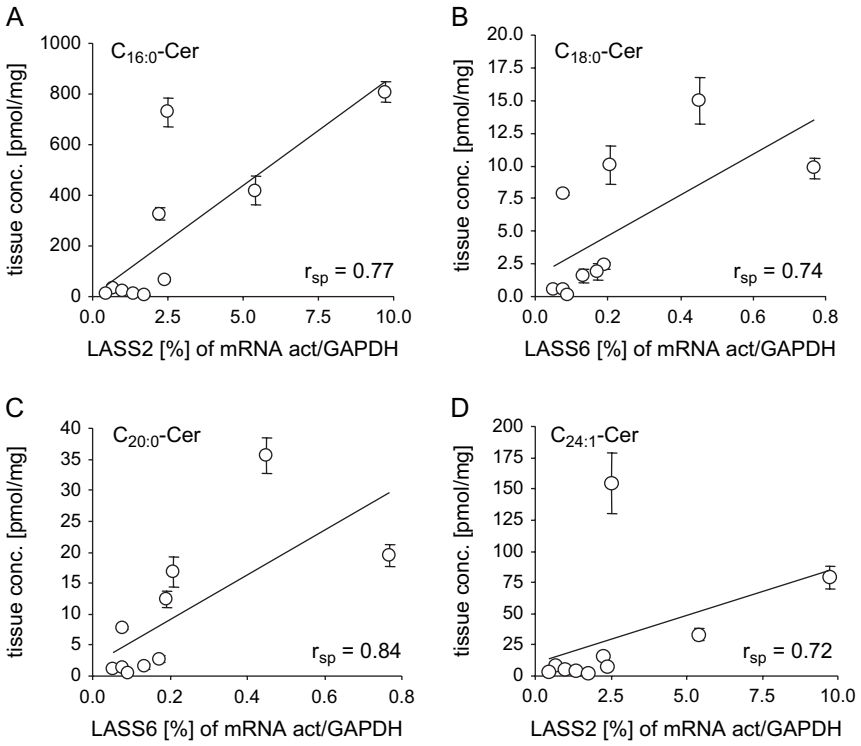

E

r_{sp}	$C_{16:0}$-Cer	$C_{18:0}$-Cer	$C_{20:0}$-Cer	$C_{24:1}$-Cer	$C_{24:0}$-Cer
LASS2	0.77	0.54	0.55	0.72	0.71
LASS4	0.48	0.65	0.68	0.62	0.47
LASS5	0.02	0.33	0.33	0.13	-0.10
LASS6	0.62	0.74	0.84	0.64	0.57
SPTLC2	0.44	0.50	0.61	0.44	0.47

Fig. 5. Linear regression analysis between the specific ceramide levels and the mRNA levels of LASS2, LASS4, LASS5, LASS6 and SPTLC2, respectively. The scatter plot shows the positive relationship between LASS2/$C_{16:0}$-Cer (**A**), LASS6/$C_{18:0}$-Cer (**B**), LASS6/$C_{20:0}$-Cer (**C**) and LASS2/$C_{24:1}$-Cer (**D**). (**E**) The table displays the Spearman's rank correlation coefficients (r_{sp}) of all combinations. The circles indicate significant correlation coefficients (circles: $P < 0.01$, dotted circles $P < 0.05$). The mRNA expression level was analyzed using real-time polymerase chain reaction. The relative expression of LASS2, 4, 5, 6 and SPT mRNA was calculated using the average mRNA levels of ß-actin and GAPDH as 100% value. Data are mean ± SEM of two experiments performed in triplicate. Each point represents one patient. A total of 10 patients with various ceramide levels were chosen.

human head and neck squamous cell carcinomas both an increase of $C_{16:0}$-Cer, $C_{24:1}$-Cer and $C_{24:0}$-Cer and a decrease of $C_{18:0}$-Cer was detected (33).

Kanto *et al.* (34) reported that supernatants of tumor cells enriched with ceramides $C_{16:0}$-Cer and $C_{24:0}$-Cer induce apoptosis in dendritic cells that helps tumor cells to escape from the immune surveillance system, indicating that an elevated ceramide level in tumor cells could also have tumor protective effects. Moreover, the increase of $C_{16:0}$-ceramide, synthesized by CerS5 or CerS6, leads to an activation of telomerase activity that is linked to tumor promotion (35). In contrary, $C_{18:0}$-Cer synthesized by CerS1, which is not expressed in breast tissue, leads to an inhibition of telomerase activity (18,35). In the here investigated breast cancer tissues, we detected elevated levels of $C_{16:0}$-Cer, $C_{24:1}$-Cer and $C_{24:0}$-Cer (Table I, Figure 3). Interestingly, the ratio between $C_{16:0}$-Cer and $C_{18:0}$-Cer increases in malignant tumor tissues ($C_{16}/C_{18} = 43$) in comparison with normal tissue ($C_{16}/C_{18} = 15$). Furthermore, the ratio between $C_{24:0}$-Cer and $C_{18:0}$-Cer increased from 5.7 (normal) to 11.8 (malignant). These data indicate that both the relationship between ceramide and phosphorylated sphingolipids [C1P (ceramide-1-phosphate), S1P] (4,6,36) as well as the relationship between ceramides of various chain lengths (especially $C_{16:0}$-Cer and $C_{18:0}$-Cer) are indicative for a proliferative or an antiproliferative status. However, we could not exclude that also S1P and C1P or other metabolites of ceramide are elevated in our tissue samples but due to low expression levels of these substances and the limited tissue amount we could not detect all sphingolipids in a sample; an objective of future studies.

Our and literature data raise the question: Are the increased ceramide levels rather an effect or a cause of malignancy? Today, we couldn't make a clear statement about this issue because our data are generated by a snap-reading method. We could not track the ceramide concentrations over the time during the development of tumors from benign to precancerous to cancerous tumors. Therefore, to elucidate whether the increased ceramide levels are a consequence or a cause of malignancy or both and whether this depends on the *N*-acyl chain length of the ceramides, further experiments are needed.

Using real-time polymerase chain reaction, we could confirm our liquid chromatography coupled with tandem mass spectrometry data, showing that the mRNA levels of LASS2, LASS4, LASS5 and LASS6

are elevated in tumor samples with high ceramide levels. In greater details, we could assign each upregulated ceramide type to one or two specific LASS isoforms (Figure 5). The data suggest that LASS2, which converts lignoceryl-CoA ($C_{24:0}$-CoA) (30) to $C_{24:0}$-Cer, also accept nervonyl-CoA ($C_{24:1}$-CoA) as a substrate. These suggestive data, however, require substantiation from further *in vitro* experiments. In contrast, we found no correlation between the expression level of SPT, the first and rate-limiting enzyme in sphingolipid *de novo* synthesis, and upregulated ceramide levels. Recently, Panjarian *et al.* also demonstrated that an increase in ceramide levels in human leukemia as well as in human colon cancer cells was mediated by induction of sphingolipid *de novo* synthesis. The effect was independent of SPT expression and activity, but rather due to an increase in CerS activity (37). In fibroblasts, the SPT translocates from the cytosol in quiescent cells to the nucleus in proliferating cells (38). The translocation would allow the enzyme to match up with the substrate and thereby inducing its activity. Therefore, translocation processes of the SPT could contribute to the raised elevated ceramide levels in the tumor tissue. It is also possible that additionally post-translational regulation processes modulate SPT activity. Last but not least, also an enhanced salvage pathway could contribute to an increase in ceramides. This has to be investigated in further studies.

Comparison of ceramide levels with pathological parameters revealed that in patients with LN metastasis $C_{16:0}$-Cer was significantly elevated. In line with our findings, Kovbasnjuk *et al.* (26) demonstrated an increase of the glycosylated ceramide Gb_3 in metastatic colon cancer tissue. Unfortunately, the study failed to specify the chain length of the ceramide backbone. Since the ER status is an important diagnostic marker in breast cancer, it is noteworthy that we observed a significant increase of $C_{18:0}$-Cer and $C_{20:0}$-Cer levels in ER positive samples as compared with ER negative samples (Figure 4B). This agrees with our previous findings where we could demonstrate by microarray analysis that the expression level of LASS4 and LASS6 are also ER status dependently regulated (14).

Moreover, we checked whether ceramide levels could be related to the clinical outcome of patients. The follow-up data of 20 patients was known. Sixteen patients were without pathological findings and six patients had a recrudescence [malignant ($n = 5$)/benign ($n = 1$)]. These included the following secondary tumor types: ovarial carcinoma ($n = 1$); mamma carcinoma ($n = 2$); osteometastasis ($n = 1$) and fibroadenoma (with a history of fibroadenoma) ($n = 1$). Five of these patients exhibited an elevated total ceramide level in their primary breast tumor sample. Only one patient with osteometastasis recrudescence showed no increase in sphingolipid level in the primary tumor sample. Due to the low patient number, no statistical significance could be achieved, but these data point to a correlation between an increased sphingolipid level and a higher risk for recrudescence.

In conclusion, in this study, we could demonstrate that ceramides $C_{16:0}$-Cer, $C_{24:1}$-Cer and $C_{24:0}$-Cer were significantly increased in malignant breast tumor tissues as compared with benign and normal tissues indicating that an increase in distinct ceramides correlates with the development of breast cancer. Furthermore, we observed a correlation between elevated ceramide levels and the ER status, whereas a raised $C_{16:0}$-Cer level was associated with a metastatic LN status.

Supplementary material

Supplements 1–5 can be found at http://carcin.oxfordjournals.org/

Funding

Deutsche Forschungsgemeinschaft Forschergruppe (FG 784/TP5); LOEWE Lipid Signaling Forschungszentrum Frankfurt.

Acknowledgements

Conflict of Interest Statement: None declared.

References

1. van Blitterswijk,W.J. *et al*. (2003) Ceramide: second messenger or modulator of membrane structure and dynamics? *Biochem. J.*, **369**, 199–211.
2. Segui,B. *et al*. (2006) Sphingolipids as modulators of cancer cell death: potential therapeutic targets. *Biochim. Biophys. Acta*, **1758**, 2104–2120.
3. Pewzner-Jung,Y. *et al*. (2006) When do Lasses (longevity assurance genes) become CerS (ceramide synthases)? Insights into the regulation of ceramide synthesis. *J. Biol. Chem.*, **281**, 25001–25005.
4. Ogretmen,B. *et al*. (2004) Biologically active sphingolipids in cancer pathogenesis and treatment. *Nat. Rev. Cancer*, **4**, 604–616.
5. Gomez-Munoz,A. (2006) Ceramide 1-phosphate/ceramide, a switch between life and death. *Biochim. Biophys. Acta*, **1758**, 2049–2056.
6. Regina Todeschini,A. *et al*. (2008) Functional role of glycosphingolipids and gangliosides in control of cell adhesion, motility, and growth, through glycosynaptic microdomains. *Biochim. Biophys. Acta*, **1780**, 421–433.
7. Dyatlovitskaya,E.V. *et al*. (2006) Role of biologically active sphingolipids in tumor growth. *Biochemistry (Mosc.)*, **71**, 10–17.
8. Taha,T.A. *et al*. (2006) Sphingosine kinase: biochemical and cellular regulation and role in disease. *J. Biochem. Mol. Biol.*, **39**, 113–131.
9. Maceyka,M. *et al*. (2005) SphK1 and SphK2, sphingosine kinase isoenzymes with opposing functions in sphingolipid metabolism. *J. Biol. Chem.*, **280**, 37118–37129.
10. Kawamori,T. *et al*. (2006) Sphingosine kinase 1 is up-regulated in colon carcinogenesis. *FASEB J.*, **20**, 386–388.
11. Johnson,K.R. *et al*. (2005) Immunohistochemical distribution of sphingosine kinase 1 in normal and tumor lung tissue. *J. Histochem. Cytochem.*, **53**, 1159–1166.
12. Pchejetski,D. *et al*. (2005) Sphingosine kinase-1 as a chemotherapy sensor in prostate adenocarcinoma cell and mouse models. *Cancer Res.*, **65**, 11667–11675.
13. Taha,T.A. *et al*. (2006) Loss of sphingosine kinase-1 activates the intrinsic pathway of programmed cell death: modulation of sphingolipid levels and the induction of apoptosis. *FASEB J.*, **20**, 482–484.
14. Ruckhaberle,E. *et al*. (2008) Microarray analysis of altered sphingolipid metabolism reveals prognostic significance of sphingosine kinase 1 in breast cancer. *Breast Cancer Res. Treat.*, **112**, 41–52.
15. Van Brocklyn,J.R. *et al*. (2005) Sphingosine kinase-1 expression correlates with poor survival of patients with glioblastoma multiforme: roles of sphingosine kinase isoforms in growth of glioblastoma cell lines. *J. Neuropathol. Exp. Neurol.*, **64**, 695–705.
16. Seelan,R.S. *et al*. (2000) Human acid ceramidase is overexpressed but not mutated in prostate cancer. *Genes Chromosomes Cancer*, **29**, 137–146.
17. Saad,A.F. *et al*. (2007) The functional effects of acid ceramidase overexpression in prostate cancer progression and resistance to chemotherapy. *Cancer Biol. Ther.*, **6**, 1455–1460.
18. Koybasi,S. *et al*. (2004) Defects in cell growth regulation by C18:0-ceramide and longevity assurance gene 1 in human head and neck squamous cell carcinomas. *J. Biol. Chem.*, **279**, 44311–44319.
19. Eto,M. *et al*. (2006) Importance of C16 ceramide accumulation during apoptosis in prostate cancer cells. *Int. J. Urol.*, **13**, 148–156.
20. Kroesen,B.J. *et al*. (2003) BcR-induced apoptosis involves differential regulation of C16 and C24-ceramide formation and sphingolipid-dependent activation of the proteasome. *J. Biol. Chem.*, **278**, 14723–14731.
21. Medler,T.R. *et al*. (2008) Apoptotic sphingolipid signaling by ceramides in lung endothelial cells. *Am. J. Respir. Cell Mol. Biol*, **38**, 639–646.
22. Yu,J. *et al*. (2007) JNK3 signaling pathway activates ceramide synthase leading to mitochondrial dysfunction. *J. Biol. Chem.*, **282**, 25940–25949.
23. Schiffmann,S. *et al*. (2009) The selective COX-2 inhibitor celecoxib modulates sphingolipid synthesis. *J. Lipid Res.*, **50**, 32–40.
24. Livak,K.J. *et al*. (2001) Analysis of relative gene expression data using real-time quantitative PCR and the 2(-Delta Delta C(T)) method. *Methods*, **25**, 402–408.
25. Kruskal,W.H. *et al*. (1952) Use of ranks in one-criterion variance analysis. *J. Am. Stat. Assoc.*, **47**, 583–621.
26. Kovbasnjuk,O. *et al*. (2005) The glycosphingolipid globotriaosylceramide in the metastatic transformation of colon cancer. *Proc. Natl Acad. Sci. USA*, **102**, 19087–19092.
27. Batheja,A.D. *et al*. (2003) Characterization of serine palmitoyltransferase in normal human tissues. *J. Histochem. Cytochem.*, **51**, 687–696.
28. Hornemann,T. *et al*. (2006) Cloning and initial characterization of a new subunit for mammalian serine-palmitoyltransferase. *J. Biol. Chem.*, **281**, 37275–37281.
29. Laviad,E.L. *et al*. (2008) Characterization of ceramide synthase 2: tissue distribution, substrate specificity, and inhibition by sphingosine 1-phosphate. *J. Biol. Chem.*, **283**, 5677–5684.

30. Mizutani,Y. *et al*. (2005) Mammalian Lass6 and its related family members regulate synthesis of specific ceramides. *Biochem. J.*, **390**, 263–271.
31. Riebeling,C. *et al*. (2003) Two mammalian longevity assurance gene (LAG1) family members, trh1 and trh4, regulate dihydroceramide synthesis using different fatty acyl-CoA donors. *J. Biol. Chem.*, **278**, 43452–43459.
32. Preetha,A. *et al*. (2005) Surface activity, lipid profiles and their implications in cervical cancer. *J. Cancer Res. Ther.*, **1**, 180–186.
33. Karahatay,S. *et al*. (2007) Clinical relevance of ceramide metabolism in the pathogenesis of human head and neck squamous cell carcinoma (HNSCC): attenuation of C(18)-ceramide in HNSCC tumors correlates with lymphovascular invasion and nodal metastasis. *Cancer Lett.*, **256**, 101–111.
34. Kanto,T. *et al*. (2001) Ceramide mediates tumor-induced dendritic cell apoptosis. *J. Immunol.*, **167**, 3773–3784.
35. Wooten-Blanks,L.G. *et al*. (2007) Mechanisms of ceramide-mediated repression of the human telomerase reverse transcriptase promoter via deacetylation of Sp3 by histone deacetylase 1. *FASEB J.*, **21**, 3386–3397.
36. Bektas,M. *et al*. (2005) Sphingosine kinase activity counteracts ceramide-mediated cell death in human melanoma cells: role of Bcl-2 expression. *Oncogene*, **24**, 178–187.
37. Panjarian,S. *et al*. (2008) *De novo* N-palmitoylsphingosine synthesis is the major biochemical mechanism of ceramide accumulation following p53 up-regulation. *Prostaglandins Other Lipid Mediat.*, **86**, 41–48.
38. Carton,J.M. *et al*. (2003) Enhanced serine palmitoyltransferase expression in proliferating fibroblasts, transformed cell lines, and human tumors. *J. Histochem. Cytochem.*, **51**, 715–726.

Received October 28, 2008; revised February 12, 2009; accepted March 7, 2009